PERFORMANCE OF ROUGHNESS CORRECTION MODELS FOR RETRIEVAL OF SEA SURFACE SALINITY FROM AIR- AND SATELLITE-BORNE L-BAND RADIOMETERS

Derek Burrage[1], Joel Wesson[1], Paul Hwang[2], and David Wang[1]

Naval Research Laboratory,
[1]Oceanography Division, Code 7300, Stennis Space Center, MS, USA
[2]Remote Sensing Division, Code 7200, DC, USA
Emails: burrage,wesson,dwang@nrlssc.navy.mil, phwang@ccs.nrl.navy.mil

1. INTRODUCTION

The launch of the European Space Agency's Soil Moisture and Ocean Salinity, SMOS, L-band microwave satellite [5] in November 2009, and the imminent launch of NASA's Aquarius satellite [13] in 2010, will allow global Sea Surface Salinity (SSS) to be mapped monthly over deep oceans with 0.2 psu precision at 100 km resolution. However, the accuracy of retrieved SSS values depend critically on methods used to correct for sea surface roughness effects. These effects change the L-band (~ 21 cm wavelength) sea surface brightness temperature, *Tb*, predicted by 'flat sea' emissivity models [11] by an amount comparable with the effects of open ocean salinity variations. Thus, they require careful correction. This paper describes the evaluation of roughness correction models designed for retrieving SSS from L-band microwave radiometer *Tb* measurements over rough seas. The paper first describes some of the wave spectrum and emission models used. Then results from several operational models are presented and compared using data from the literature and recent NRL Salinity, Temperature and Roughness Remote Scanner, STARRS, airborne salinity mapper [1] campaigns.

2. METHODS

2.1. Wave Spectral Models: The dominant roughness influence on SSS retrieval comes from the shorter (1cm-1m) Bragg-scale components of the wind-wave spectrum. These waves are rarely represented in conventional spectrum models, which must be modified to account for their effects ([8] [12]) when used in roughness emission modeling. These components are modulated by long waves, so they are also influenced by swell [7].

2.2. Roughness Emission Models: Various roughness emission models are presently available or under development, to correct for the adverse effects of roughness-enhanced emission on microwave SSS retrievals. These include rigorous [14], asymptotic [10] [15] [17] and empirical model types [2] [6]. Several models of the

last two types are implemented in the SMOS Level 2 processor. The asymptotic models are driven by auxiliary wind data and are based on a specified wind-wave spectrum. Their accuracy is strongly influenced by the choice of spectrum. The empirical models are driven directly by auxiliary wind or sea state data, and calibrated using in situ observations. They take advantage of SMOS's multi-angle view capability [5]. In contrast, Aquarius will model roughness empirically using radar cross sections observed by an on-board L-band scatterometer [13]. The variety of models adopted, even for the single mission, SMOS, is a reflection of recent issues and innovations in this field, and of the dominant role of sea surface roughness corrections in the L-band radiometer error budgets.

3. RESULTS

To investigate the importance of model choice in computing roughness corrections for SSS retrieval, we compared results from the Two-Scale Model (TSM) of Yueh [17] and Reul's (pers. comm.) version of the SPM/SSA asymptotic model [10][15], both of which are implemented in the SMOS L2 processor. These models also employ different wind-wave spectra to describe sea roughness. SPM/SSA is driven by the Kudryavtsev, et al. spectrum [12] and TSM by the Durden-Vesecky spectrum (multiplied by a factor of two), with Gaussian-distributed long wave slopes [17]. A significant difference in the *Tb*'s predicted by TSM versus the SPM/SSA model appeared, particularly for H-Pol. At 50 deg. incidence angle, TSM predicts ~ 2 K lower *Tb* influence than SPM/SSA (~4 psu SSS error!). Such under-prediction has previously been reported by others.

To illustrate the effect of spectrum choice for a single asymptotic roughness correction model, we show two surface curvature spectra (Fig. 1) and resulting predictions of L-band H-Pol *Tb*'s, both derived using Reul's implementation of the SPM/SSA model. The input wave spectra were those of Kudryavtsev et al. (K) [12] and Elfouhaily et al. (E) [4]. The resulting *Tb* predictions differ by ~ 1 K for an SSS error of about 2 psu under typical temperate conditions (V-Pol errors, not shown, were similar). Comparison of *Tb* sensitivity to wind which results from using E and K, along with the Donelan (D) [3] and Hwang (H) [8] spectrum to drive SPM/SSA (Fig. 2) shows that H performs best for H-Pol *Tb* and is competitive with K for V-Pol, considering field data spread.

A STARRS transect crossing the continental shelf and western half of the Gulf Stream conducted during NRL's VIRGO experimental campaign in Dec., 2006 (Fig 2.) shows SST's obtained from the STARRS and MODIS IR radiometers and Gulf Stream location (Left panels), and the corresponding STARRS SSS transect (right panel). The bar chart (lower right) shows the V-Pol *Tb* corrections (Delta *Tb*) computed from TSM, the empirical WISE emissivity model [2] (WS), and SPM/SSA, at locations near NDBC data buoys. The wind speeds observed by the buoys during the flight are also shown. The corresponding SSS correction in this region, in psu, is approximately 2 x Delta *Tb* (K). TSM consistently under-predicts Delta *Tb* with respect to SPM/SSA across the whole range by a factor of about 2. Implied model-dependent errors are of order 0.75 K in this case,

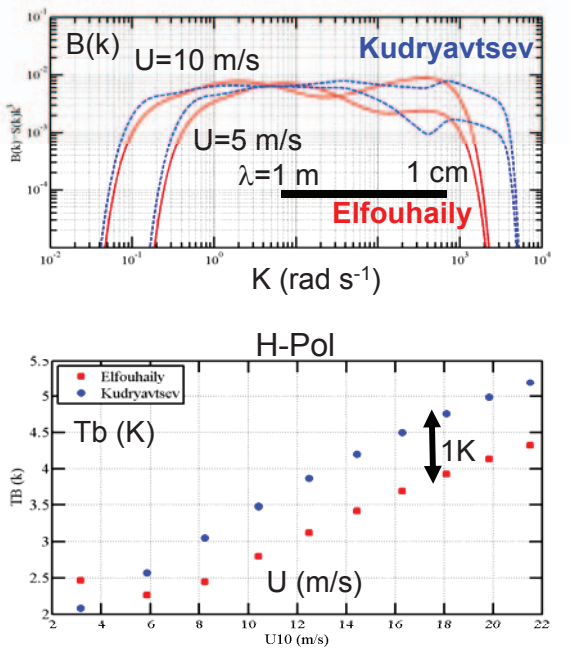

Fig 1. SPM/SSA calculations from different wind-wave Spectra. (Top) Curvature spectra of Elfouhaily et al. [3] and Kudryavtsev et al. [9]. (Bottom) Predicted *Tb*'s from SSA/SPM , Inc. Ang. 37 deg., *Ts* 298 K, *S* 35 psu, Inv.wave age=0.84.

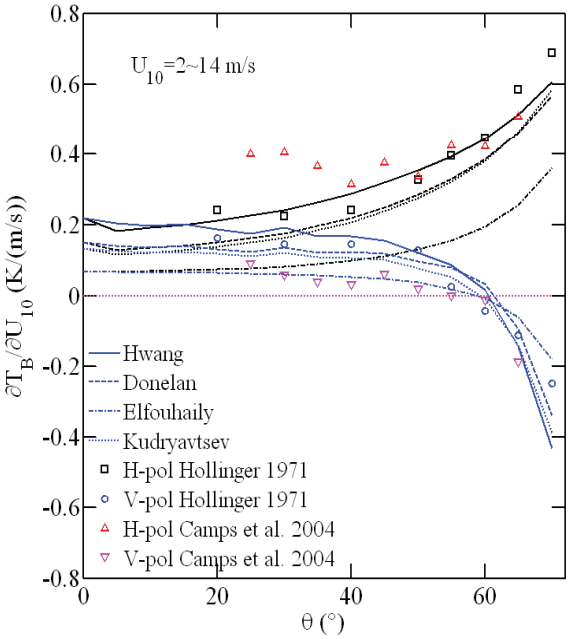

Fig 2. Average rate of change of *Tb* with respect to wind speed ($\partial Tb/\partial U_{10}$) at 1.41 GHz calculated using four different wind-wave spectra for wind speed range 2 to 14 m/s. *Hollinger* [1971] and *Camps et al.* [2004] field data superimposed. [Adapted from Hwang et al., 2010]

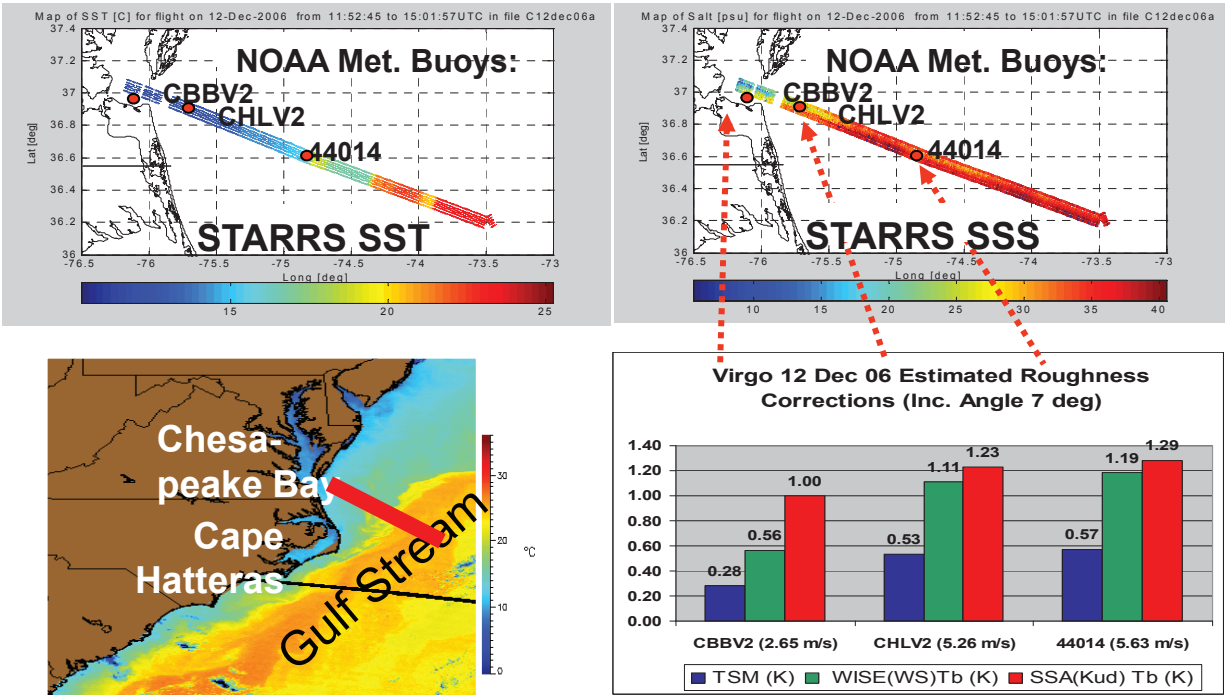

Fig 3. (Top) STARRS SST and SSS transect from Chesapeake Bay entrance to mid Gulf Stream passing NDBC buoys. (Lower left) MODIS satellite SST image showing transect crossing Gulf Stream. (Lower right) Bar chart showing L-band *Tb* [K] corrections from TSM (blue), WS (green), and SPM/SSA (red) for the buoy locations, and observed wind speeds [m/s] (see labels).

corresponding to an SSS correction error of about 1.5 psu. This error can be compared with an SSS difference of ~5 psu observed across the Gulf Stream in 1999, using the PALS L-band microwave radiometer [16].

4. CONCLUSIONS

We conclude that it is vital to choose the roughness correction model and input forcing function (wind speed, or spectrum) carefully to minimize this major error source for L-band SSS retrieval. Further comparisons with *Tb* corrections estimated from the TSM and SPM/SSA models in application to both STARRS and SMOS data are presently being carried out. The results will be compared with a rigorous FDTD reference model, which is currently under development, and they will be shared with the ESA SMOS and NASA Aquarius science teams.

5. REFERENCES

[1] D. M. Burrage, et al., "Optimizing performance of a microwave salinity mapper," *JAOT*, 25 (5), pp 776-793, 2008.

[2] A. R. Camps, et al., "Sea Surface Emissivity at L-Band: Derived Dependence with incident and azimuth angles". Proc. of *First Results Workshop on EuroSTARRS, WISE, LOSAC Campaigns*, CESBIO, Toulouse, FR, 4-6 Nov. 2002, ESA SP-525, pp. 105-116, 2003.

[3] M. A. Donelan, et al., "Directional spectra of wind-generated waves", *Phil. Trans. Roy. Soc. Lond.*, A315,509-562, 1985.

[4] T. Elfouhaily, et al., "A unified directional spectrum for long and short wind-driven waves", *JGR*, 102 (C7), pp 15781-15796, 1997.

[5] J. Font, et al., "The determination of surface salinity with the European SMOS space mission," *TGRS*, 42 (10), pp. 2196-2205, 2004.

[6] C. Gabarro, et al. "Use of empirical sea surface emissivity models to determine sea surface salinity from an airborne L-band radiometer," *Scientia Marina*, June, 72 (2), pp 329-336, 2008.

[7] P. A. Hwang, "Observations of swell influence on ocean surface roughness," *JGR*, 113, C12024 pp 1-14, doi:10.1029/2008JC005075, 2008.

[8] P. A. Hwang, "Wave number spectrum and mean-square slope of intermediate-scale ocean surface waves", *JGR*, 110, C10029, doi:10.1029/2005JC003002, 2005.

[9] P. A. Hwang, D. M. Burrage, D. W.-C. Wang and J. C. Wesson, " A study on the influence of ocean surface roughness spectral models on microwave brightness temperature computation" *JGR* (In Review)

[10] J. T. Johnson and Min Zhang, "Theoretical Study of the Small Slope Approximation for Ocean Polarimetric Thermal Emission," *TGRS*, 37 (5), pp 2305-2316, 1999.

[11] L. Klein, and C. Swift, "An improved model for the dielectric constant of sea water at microwave frequencies," *TAP* 25 (1), pp 104-111, 1977.

[12] V. Kudryavtsev, D Hauser, G Caudal, B Chapron, "A semi-empirical model of the normalized radar cross section of the sea surface, 1. Background model," *JGR*, 108 (C3), 8054, doi:10.1029/2001JC001003, 2003.

[13] G. Lagerloef, "The Aquarius/SAC-D Mission.*Oceanography,"* 21 (1), pp 68-81, 2008.

[14] N. Reul, et al. "On the Use of Rigorous Microwave Interaction Models to Support Remote Sensing of Natural Surfaces" *IGARSS 2005*, Proc. 3, pp 2195-2198, 2005.

[15] Voronovich, A. G., *Wave Scattering from Rough Surfaces*, Berlin: Springer-Verlag, 1994.

[16] W. J. Wilson, et al., "Ocean surface salinity remote sensing with the JPL Passive/Active L-/S-band (PALS) Microwave Instrument", *IGARRS 2001,* Sydney, Australia. 2, pp 937-939, 2001.

[17] S. Yueh, "Modeling of wind direction signals in polarimetric sea surface brightness temperatures," *TGRS*, 35 (6) pp 1400–1418, 1977.